International Journal of Nanomedicine

Dovepress
open access to scientific and medical research

Open Access Full Text Article

ORIGINAL RESEARCH

# Nano Parthenolide Improves Intestinal Barrier Function of Sepsis by Inhibiting Apoptosis and ROS via 5-HTR2A

Ning-Ke Guo[1,2,*], Han She[1,*], Lei Tan[1], Yuan-Qun Zhou[1], Chun-Qiong Tang[1], Xiao-Yong Peng[1], Chun-Hua Ma[1], Tao Li[1], Liang-Ming Liu[1]

[1]State Key Laboratory of Trauma, Burns and Combined Injury, Shock and Transfusion Department, Research Institute of Surgery, Daping Hospital, Army Medical University, Chongqing, People's Republic of China; [2]The Third Affiliated Hospital of Xinxiang Medical University, Xinxiang, People's Republic of China

*These authors contributed equally to this work

Correspondence: Tao Li; Liang-Ming Liu, Email lt200132@163.com; lmliu62@tmmu.edu.cn



**Background:** Intestinal barrier dysfunction is an important complication of sepsis, while the treatment is limited. Recently, parthenolide (PTL) has attracted much attention as a strategy of sepsis, but whether nano parthenolide (Nano PTL) is therapeutic in sepsis-induced intestinal barrier dysfunction is obscured.

**Methods:** In this study, cecal ligation and puncture (CLP)-induced sepsis rats and lipopolysaccharide (LPS)-stimulated intestinal epithelial cells (IECs) were used to investigate the effect of PTL on intestinal barrier dysfunction. Meanwhile, we synthesized Nano PTL and compared the protective effect of Nano PTL with ordinary PTL on intestinal barrier function in septic rats and IECs. Network pharmacology and serotonin 2A (5-HTR2A) inhibitor were used to explore the mechanism of PTL on the intestinal barrier function of sepsis.

**Results:** The encapsulation rate of Nano PTL was 95±1.5%, the drug loading rate was 11±0.5%, and the average uptake rate of intestinal epithelial cells was 94%. Ordinary PTL and Nano PTL improved the survival rate and survival time of septic rats, reduced the mean arterial pressure and the serum level of inflammatory cytokines, and protected the liver and kidney functions in vivo, and increased the value of transmembrane resistance (TEER) reduced the reactive oxygen species (ROS) and apoptosis in IECs in vitro through 5-HTR2A. Nano PTL had better effect than ordinary PTL.

**Conclusion:** Ordinary PTL and Nano PTL can protect the intestinal barrier function of septic rats by inhibiting apoptosis and ROS through up-regulating 5-HTR2A, Nano PTL is better than ordinary PTL.

**Keywords:** sepsis, nano PTL, intestinal permeability, 5-HTR2A, apoptosis

## Introduction

Sepsis refers to life-threatening organ dysfunction caused by the imbalance of the body's response to infection. It is a typical critical illness in Intensive Care Unit (ICU) with high incidence and mortality. According to statistics in 2017, there are 48.9 million sepsis patients worldwide every year. The mortality rate is as high as 20–30%.[1] So far, sepsis is still a huge challenge threatening human life safety. Intestinal barrier function plays a vital role in sepsis. Under normal circumstances, the intestinal barrier can effectively block pathogens from entering the internal environment. During sepsis, the intestinal barrier is injured, which can lead to the translocation of intestinal flora and endotoxin, aggravating the sepsis process and causing multiple organ dysfunction and even death.[2] The protection of intestinal barrier function has attracted more attention in the treatment of sepsis. Protecting the intestinal barrier and reducing intestinal permeability have important clinical significance for preventing and treating of sepsis.[3] The current conventional treatment measures for sepsis mainly include fluid resuscitation, antimicrobial, anticoagulation drug therapy, organ function support

Received: 23 October 2022
Accepted: 2 February 2023
Published: 11 February 2023

and so on. However, the protective effects on intestinal barrier function are not predicted,[4] so it is urgent to find a new approach that can effectively protect the intestinal barrier function of sepsis.

In recent years, the protective effect of traditional Chinese medicine on sepsis organ function has attracted extensive attention. Parthenolide (PTL) is a sesquiterpene lactone compound purified from the traditional Chinese medicine chamomile. It belongs to terpenoids and has a wide range of pharmacological and biological activity.[5] In recent years, studies have found that PTL has a good anti-inflammatory effect and has an important protective effect on liver ischemia-reperfusion injury, cerebral ischemia, and other diseases.[6,7] It inhibits the expression of inflammatory-related genes and proteins in the JAK2/STAT3 signaling pathway that alleviates liver ischemia-reperfusion injury.[8] Its lipophilicity is conducive to good blood–brain barrier (BBB) permeability by increasing the levels of superoxide dismutase (SOD) and chloramphenicol acetyltransferase (CAT), reducing the level of malondialdehyde (MDA), down-regulating the expression of TLR4 and NF-κB, and increasing the level of claudin-5 protein expression to play a role in brain protection.[9] Another study reported that PTL could significantly improve hypotension in septic rats.[10] In addition, studies found that PTL could block the phosphorylation and subsequent degradation of IκB protein, significantly reduce the severity of dextran sodium sulfate (DSS)-induced colitis and led to downregulation of MPO activity and phosphorylated NF-κB p65 expression to ameliorate colonic inflammation in sepsis mice.[11] While whether PTL has a protective effect on the intestinal barrier function in septic rats needs to be further studied.

Most traditional Chinese medicines are limited in clinical application due to their strong hydrophobicity, poor stability, low bioavailability, short half-life in vivo and so on. Nanosizing of traditional Chinese medicines is not to produce the new drugs but to develop the advantages of nano dosage form, including enhancing the pharmacological activity, achieving the targeted drug delivery, improving the bioavailability, and reducing the toxicity.[12] Nano-drugs have been a research hotspot in recent years. Recent studies found that nano-drugs can enhance their solubility, for instance, lipidic cubic-phase leflunomide nanoparticles can increase their diffusion rate into cells, and improve the drug distribution, thereby enhancing their efficacy and anti-inflammatory effects.[13] Nano-realgar can improve its bioavailability and cell uptake rate, and the effect of nano-realgar is better than ordinary realgar at the same dose.[14] It is widely used in clinical practice because of its excellent stability, high drug loading rate, good sustained drug release profile, and solubility of drug and bioavailability.[15] Previous studies have found that nano-drugs can interact with the plasma membrane in the extracellular environment and enter into the cells through endocytosis.[16] The endocytosis efficiency of cells includes the size, surface charge, and surface coating of the drug. The smaller the particle size of nano-drugs, the easier it is to be endocytosed. Cells have a higher uptake rate of nano-drugs with smaller particle sizes, thereby increasing their therapeutic effect.[17] Previous studies have also found that the efficacy of nano-drugs is better than that of ordinary drugs.

In this study, we used cecal ligation and puncture (CLP) and lipopolysaccharide (LPS)-stimulated intestinal epithelial cells (IECs) in vivo and vitro to observe the effect of Nano PTL on the intestinal barrier function of sepsis. We find a new therapeutic method for the prevention and treatment of sepsis.

# Materials and Methods

## Ethical Approval of the Study Protocol

The study protocol was approved by the Research Council and Animal Care and Use Committee of Research Institute of Surgery, Daping Hospital, Army Medical University (Chongqing, China; approval number SYXK-20170002). The investigation conformed to the Guide for the Care and Use of Laboratory Animals published by the US National Institutes of Health (8th edition, 2011, National Institutes of Health, Bethesda, MD).

## Reagent

LPS (Cat. L8274), ATP (Cat. A2383-10G), and Evans blue (Cat. E2129-10G) were purchased from Sigma company (USA). PTL (Cat. 20554-84-1) was purchased from Santa Cruz company (USA). ELISA kits of IL-1β (Cat. E-EL-R0012c), IL-6 (Cat. E-EL-R0015c), D-lactic acid (Cat. E-BC-K002-M), TNF-α (Cat. E-EL-R2856c) were purchased from Elabscience company (China). Dulbecco's Modified Eagle Medium (DMEM) (Cat. C11995500BT) was

purchased from Gibco company (USA). Antibodies for ZO-1 (Cat. PB9234), β-actin (Cat. BM0627) and PBS powder (Cat. AR0030) were purchased from Boster (China). Antibodies for 5-HTR2A (Cat. bs-20743R), PKC (Cat. bs-3531R) were purchased from Bioss (China). Antibodies for Bax (Cat.14796S), CytC (Cat.11940S). cleaved-Caspase3 (Cat.9664S) were purchased from Cell Signaling Technology company (USA). ROS kit (Cat. S0033S) was purchased from Beyotime Biotechnology (China). FITC Annexin V Apoptosis Detection Kit (Cat.556547) was purchased from BD company (USA). Transwell 6-well culture plate (Cat.3470-Clear) was purchased from Costar company (USA). EVOM2 Cell transmembrane resistance test was purchased from World Precision Instruments company (USA). DAPI (Cat. ab188804) was purchased from Abcam company (USA). Secondary antibody goat anti-rabbit, anti-mouse IRDye 800CW (Cat. ab216772, ab216773) were purchased from Odyssey company (USA). Acetonitrile (Cat.75-05-8) was purchased from Burdick & Jackson company (USA), column (5μm C18,150×4.6mm, Cat.81001) was purchased from Dikma company (China), fluoresceinIsothiocyanate (FITC) (Cat.27072-45-3) was purchased from aladdin company (China), and risperidone (Cat. HY-11018) was purchased from MedChemExpress company (China).

## Preparation of Nano PTL

Nano PTL was prepared using Kolliphor HS-15 (surfactant), polyethylene glycol (PEG-400: co-surfactant), and medium-chain triglycerides (MCT: oil) at the ratio of 4:2:1 (w/w/w). PTL was dissolved in MCT, then mixed with HS-15 and PEG-400, followed by gently stirring using a magnetic stirrer at 300 rpm for 30 min at 25°C. After equilibrium at room temperature for 30 min, the solution was diluted 100-fold with double-distilled water and stirred till clear and slightly bluish.

## Characterization of Nano PTL

The droplet size, zeta potential (ZP), and polydispersity index (PDI) were measured by a Zetasizer Nano ZS based on dynamic light scattering at 25 °C. The morphology of Nano PTL was determined by Hitachi-HT7700 transmission electron microscope. Samples with a 500-fold dilution were placed on a copper grid (400 mesh). After the samples were dried, they were stained with phosphor tungstic acid (2%) for 30s at room temperature to form a thin film and then observed under the transmission electron microscope (TEM). According to the energy-level transition caused by the absorption of radiation energy, the infrared absorption spectrum of the molecule is obtained by recording the transition process (infrared spectroscopy).

## Determination of Nano PTL Encapsulation Efficiency and Drug Loading

Blank control solution: The lipids and surfactants lacking PTL were taken, and the blank sample was prepared according to the preparation method of Nano PTL. An appropriate amount of the sample was dissolved in acetonitrile and filtered by a microporous filter membrane (0.45μm). Reference solution: A proper amount of each reference was accurately weighed, dissolved in acetonitrile, and diluted in multiple proportions. Sample solution: An appropriate amount of Nano PTL dissolved in acetonitrile was taken, filtered by a microporous filter membrane (0.45μm) to obtain. Linear relationship investigation: The appropriate amount of the above reference solution was precisely absorbed and analyzed by injection. The analysis results were regressed with the injection mass (X, μg) of the reference by the peak area (Y). Determination of free supernatant (WF): A small amount of sample solution was carefully absorbed, placed in a centrifuge tube, centrifuged (14000r/min) for 30min, the supernatant was absorbed, and injected into the chromatograph for analysis. The total dosage (WT) of Nano PTL determination: 2.5 μg sample solution was taken, filtered by microporous filter membrane (0.45 μm), and injected into the chromatogram for analysis. the encapsulation rate and drug load of each component were calculated respectively, according to the formulae: $\text{Encapsulationrate} = (\text{WT} - \text{WF})/\text{WT} \times 100\%, \text{drugload} = (\text{WT} - \text{WF})/\text{WS} \times 100\%$ (WS is the total amount of carrier materials and drugs). Chromatographic column: Acetonitrile–ultrapure water as mobile phase, gradient elution; The flow rate of 1.0 mL/min; Column temperature: 40 °C; Sample quantity: 10 μL; Detection wavelength: 210nm.

## Uptake Percentage of PTL and Nano PTL

PTL and Nano PTL containing FITC 1μmol/L were respectively added to the intestinal epithelial cells in the 96-well culture plate after pre-culture and adhesion growth. After incubation for 1h, 2h, 4h, 8h and 12h, the cells were washed twice with phosphate-buffered saline (PBS) and digested by trypsin. The fluorescence intensity of the cell suspension was measured at 485 nm by a microplate reading instrument. Uptakepercentage(%)= $Z/Z_0 \times 100\%$, where Z is the fluorescence intensity of cell suspension measured at different sampling times, and $Z_0$ is the fluorescence intensity of cell suspension added with FITC.

## Sepsis Model of Rats

Adult SD rats (weight 200–220g, provided by the experimental animal center of Daping Hospital of Army Medical University) were anesthetized by intraperitoneal injection of sodium pentobarbital (45 mg/kg). SD rats were fasted for 8 hours before the operation and given water freely. Cecal ligation and puncture (CLP) were used to replicate the sepsis model in rats. Briefly, the abdomen was disinfected routinely and cut the skin straight along the abdomen to expose the cecum. Ligated the cecum at 0.7 cm away from the distal end (needle diameter 1.5mm), pushed the feces gently toward the distal cecum, and perforated the cecum's end with a conical device. The feces naturally flowed into the abdominal cavity. Then, the cecum was relocated, the wound was sutured layer by layer, and sterile normal saline was injected intraperitoneally at 2mL/100g. The animals were put back to the cage to access to water freely but not food. Twelve hours after the operation, the femoral artery was intubated to monitor the mean arterial blood pressure (MAP). The CLP model was established successfully when the MAP decreased by 30%.[18]

## Experimental Protocol

### In vivo Experiments

Eighty SD rats were randomly divided into five groups: Normal control (Sham), sepsis (Sep), conventional treatment (CT), parthenolide (PTL), and nano parthenolide (Nano PTL). Sham group: Only open and close abdomen; sepsis group: Cecal ligation and puncture to make sepsis model; conventional treatment group: 12 hours after making sepsis model, lactated Ringer's 35 mL/kg + dopamine 5–10 μg/(kg·min) were infused through the femoral vein, infusion for 3 hours, and intramuscular injection of cefuroxime sodium 100 mg/kg at the same time to maintain MAP>70 mmHg; parthenolide group: 30 minutes before CLP establishment, parthenolide was given via tail vein 5 mg/kg, 12 hours after the sepsis model was made. Then, we gave parthenolide 5 mg/kg on the basis of conventional treatment; the nano parthenolide group was given the same dose as the parthenolide group. Sixteen rats in each group were used to observe the survival time and rate of rats, and 8 rats were used to observe the blood pressure of rats. In a subsequent experiment, 40 SD rats were randomly divided into five groups: Normal control (Sham), sepsis (Sep), conventional treatment (CT) group, parthenolide (PTL), nano parthenolide (Nano PTL), and used to detect blood inflammatory cytokine levels, intestinal tissue Evans Blue content, blood D-lactic acid level, intestinal pathological morphology and liver and kidney function.

### In vitro Experiments

We took intestinal epithelial cells that were obtained from the American Type Culture Collection (ATCC, Manassas, VA, United States) and cultured them in DMEM supplemented with 10% FBS in a humidified, 5% $CO_2$/95% air atmosphere at 37°C after 3–5 generations, then they were divided as normal control (Normal), LPS, PTL and Nano PTL group. Normal group: the culture medium was changed to a serum-free basal medium 12h before the experiment; LPS group: The serum-free basal medium was added with 1μg/mL LPS to incubate for 12 h, and then 5 mmol/L adenosine-triphosphate (ATP) was added to incubate for 2 h; PTL group: 1 μmol/L PTL was added to the serum-free basal medium and incubated for 30 min, and then 1μg/mL LPS was added. They were incubated for 12h, then 5mmol/L ATP and 1μmol/L PTL were added to incubate for 2h; Nano PTL group: 1μmol/L Nano PTL was added to serum-free basal medium for 30 min incubation, then 1μg/mL LPS was added to incubate for 12h, and then added 5mmol/L ATP and 1μmol/L Nano PTL were incubated for 2h. The fluorescence expression of ZO-1, transmembrane resistance, and protein expression of protein kinase C (PKC), zonula occludens-1 (ZO-1), and 5-HTR2A in intestinal epithelial cells of each group were measured. 5-HT Inhibitor group: 1μmol/L Nano PTL was added to the serum-free basal medium and

incubated for 30 min, then 1μg/mL LPS and risperidone (4.8 nmol/L)[19] were added to incubate for 12h, and then 5 mmol/L ATP and 1μmol/L Nano PTL were added to incubate for 2h. The ROS, apoptosis level, protein expression of BCL2-associated x (Bax), Cytochrome (CytC), cleaved-Caspase3, and transmembrane resistance were measured in each group.

## Detection of Survival Rate and Mean Arterial Pressure

After 12 h of CLP, the femoral vein fluid was resuscitated, and the femoral artery cannula was inserted simultaneously to record the rats' arterial blood pressure with an arterial sphygmomanometer, which was recorded every 30 min until the end of 150 min. Blood pressure was recorded by directly inserting the femoral artery into the sepsis group.

After fluid resuscitation, the femoral vein of the rat was cannulated and ligated, and then the wound was sutured. The rats were returned to the cage and fed with a normal diet and water. They were observed once an hour until 48 h after resuscitation, and the survival time of the rats was recorded.

## Determination of Blood Inflammatory Cytokine Levels

After 12 h of CLP, 2 mL abdominal aortic blood of rats was drawn, placed at room temperature for 30 min, and centrifuged at 1000×g for 20 min. The upper serum was collected, and a standard substance or sample was added to each well of the ELISA strip. The concentrations of interleukin-6 (IL-6), interleukin-1β (IL-1β), and tumor necrosis factor-α (TNF-α) in the blood of rats were determined by the ELISA method.

## Detection of Liver and Kidney Function in Rats

After 12 hours of CLP model, 2mL of rat abdominal aorta blood was taken and left at room temperature for 20 min, 3000 r/min, centrifuged for 10 min to detect activity of aspartate aminotransferase (AST), alanine aminotransferase (ALT), urea nitrogen (Urea) and creatinine (Crea) with automatic biochemical analyzer.

## Determination of Intestinal EB Content

Normal rats were anesthetized with 30 mg/kg, and rats in the other groups were anesthetized by intraperitoneal injection of 15 mg/kg of sodium pentobarbital. The abdominal cavity was opened, and a section of the small intestine was taken to prepare an intestinal pouch. The intestinal cavity was washed until the washing liquid was clear, dried, and added to formamide solution. The absorbance was measured at 650 nm on a microplate reader to calculate the EB content per gram of dry intestinal weight to reflect the intestinal permeability.

## Blood D-Lactic Acid Content Detection

Twelve hours after the CLP model, 2 mL of rat abdominal aortic blood was collected, placed at room temperature for 20 min, and centrifuged at 3000 r/min for 10 min. The upper serum was collected, and the serum D-lactic acid concentration was measured by D-lactic acid kits to reflect intestinal permeability.

## HE Staining

SD rats were fixed by intraperitoneal anesthesia. The abdomen was opened, and the intestinal segment of 6–7 cm was taken. The blood stained on the surface was washed with PBS solution on ice and fixed with 4% paraformaldehyde solution for 48–72 h. After the fixation time, the intestinal tissue was taken out. The tissues were cut into small pieces with a thickness of 2–3 mm, placed in a dehydration box to rinse with slow water flow overnight, and then carried out the operations of transparency, immersion in wax, embedding, sectioning, and staining. The coverslips were dried and observed under an optical microscope.[20]

## Immunofluorescence

After the drug treatment, we poured out the cell culture medium. The cells were collected and fixed with 4% formaldehyde at −20°C for 10 min. And then, 0.1% Triton permeabilized for 5 min. Goat serum was added and incubated at room temperature for 10 min, and ZO-1 primary antibody (1:200) was added, stayed overnight at 4 °C,

then incubated with secondary antibody (1:200) at 37 °C for 30 min, then added DAPI (1:100) and incubated at 37 °C for 10 min in the dark. Then, the expression of ZO-1 was observed under a laser confocal microscope.

## Western Blot

Cell level: Three to five generations of intestinal epithelial cells were cultured to 80% confluence, added 1μg/mL LPS, 5mmol/L ATP, 1μmol/L PTL or Nano PTL and collected cells to extract the total proteins. Animal level: SD rats were anesthetized by intraperitoneal anesthesia, the abdomen was opened, a small amount of intestinal segment was taken, the stained blood was washed with PBS solution on ice, the protein was extracted and conducted by electrophoresis, the target protein was transferred to PVDF membrane, and sealed with 5% non-fat milk powder for 1 h, washed with goat antibody, and then added goat antibody. Rat β-actin antibody (diluted 1:1000) and rabbit anti-rat antibody (diluted 1:1000) were used and incubated at 4°C overnight, and then incubated with goat anti-rabbit IR Dye 800CW secondary antibody at room temperature for 1 h, after washing 3 times, the Odyssey Clx infrared imager was used to scan the membrane, the bands were analyzed by ImageJ software to detect protein expression of PKC, ZO-1, Bax, CytC, cleaved-Caspase3 and 5-HTR2A in intestinal epithelial cells of each group.

## Using Network Pharmacology to Predict the Target of PTL

The SMILES number of parthenolide in the PubChem (http://pubchem.ncbi.nlm.nih.gov/) database was found to put it into the Swiss Target Prediction (http://www.swisstargetprediction.ch) database for predicting PTL Target gene; Genecards (http://www.genecards.org) database was used to screen the pathological sepsis targets with higher score values. The Venn diagram was used to take their intersection to get the potential targets of PTL regulating sepsis. The obtained potential targets were analyzed for enrichment (Kyoto Encyclopedia of Genes and Genomes, KEGG). We selected two pathways related to this study: Inflammatory mediator regulation of TRP channels and gap junction-enriched genes to make a Venn diagram.

## Measurement of Transmembrane Resistance of Intestinal Epithelial Cells

Intestinal epithelial cells from 3 to 5 generations were inoculated into a 6-well transwell culture plate, $1\times10^5$ cells/mL. When the cells grew to 80% confluent, 1μg/mL LPS, 5mmol/L ATP, 1μmol/L PTL or Nano PTL were added. The transmembrane resistance value of intestinal epithelial cells was measured within 12 hours. The specific method was carried out according to the EVOM2 operation manual. The wells without cells were set as blank control, and the transmembrane resistance value of cells = (measured resistance value - blank resistance value) ×transwell effective membrane area, the unit is $\Omega\cdot cm^2$.

## ROS Level Determination

The 3–5 generations of intestinal epithelial cells were inoculated into confocal dishes, when the cells grew to 80% confluent, 1μg/mL LPS, 5mmol/L ATP, 1μmol/L PTL or Nano PTL, and DCFH-DA were added. After incubation for 45 min, ROS levels in each group were observed under a laser confocal microscope.

## Flow Cytometry Apoptosis Detection

The 3–5 generations of intestinal epithelial cells were inoculated into the culture flask when the cells grew to 80% confluent, 1μg/mL LPS, 5mmol/L ATP, and 1μmol/L drugs were added, and the cells were digested with trypsin. After 12 h, the cells were collected and washed with ice-cold PBS buffer, then resuspended the cells in 1× Binding Buffer at a concentration of $1\times10^6$cells /mL; Then took 100 μL into the EP tube, added FITC Annexin V and propidium iodide (PI), and rotated the cells gently. Finally, the cells were incubated in the dark at room temperature for 15 min, and 400 μL of 1× binding buffer was added to each tube and analyzed by flow cytometry within 1 h.

## Statistical Analysis

Statistical analysis was performed using SPSS 17.0 (SPSS Inc., Chicago, Illinois, USA). Data are presented as mean ± standard deviation of results from at least three independent experiments. One-way analysis was performed using variance and post hoc tests (S-N-K/LSD). Values of $P<0.05$ mean statistically significant.

# Results

## Characterization of Nano PTL

Nano parthenolide (Nano PTL) micelles have been verified by NMR and mass spectrum (Figure 1A and B). δ3.4 represented the ester bond of Nano PTL, δ2.51 represented the characteristic peak of epoxy group of Nano PTL, δ4.62 represented the characteristic peaks of methyl group of Nano PTL. δ216 represented the characteristic peaks of methylene of Nano PTL. The electron microscope showed that Nano PTL was spherical with regular particles. Under the transmission electron microscope, Nano PTL was displayed as microemulsion droplets (Figure 1C). The average particle size of Nano PTL was (108.6±0.8) nm, and the zeta potential was (−17±0.6) mV (Figure 1D and E), the parthenolide-C=O-O- infrared spectral feature was at 3406.40 $cm^{-1}$, and showed a large wide peak, which is a carbon-based characteristic peak. -CH2- peak appeared at 2872.58 $cm^{-1}$, and presented tooth shaped double peaks. This is the characteristic peak of methylene. In addition, the epoxy group peak of the key active group of parthenolide lactone appeared at 1108.38 $cm^{-1}$. The results showed the characteristic group of parthenolide had featured absorption peak (Figure 1F). The regression equation of PTL was Y=3614600X+47566, the encapsulation rate of Nano PTL was 95 ±1.5%, and the drug load was 11±0.5% (Supplementary Figure 1A–C). The uptake rate of Nano PTL by intestinal epithelial cells was higher than ordinary PTL, the peak time of uptake was at 8h, the average uptake rate of Nano PTL was 94%, while the average uptake percentage of ordinary PTL was 87%. Under the confocal microscope, the fluorescence intensity was the strongest at 8h (Figure 1G and H).

## Protective Effect of Nano PTL on Sepsis Rats

The 24h survival rate of the rats in the sepsis group was 0, and the 24h survival rate of the rats in the conventional treatment group was 12.5%. In the ordinary PTL group, 7 rats of 16 rats survived for 48 h, the 48h survival rate was 43.6%, the average survival time was 29 h. In the Nano PTL group, the 48h survival rate of sepsis rats was 62.5%, and the average survival time was 45 h. The results showed that both ordinary PTL and Nano PTL could significantly improve the survival of sepsis rats. Nano PTL had better effect (Figure 2A and B). Compared with the normal group, the serum levels of IL-6, IL-1β and TNF-α in sepsis rats were significantly increased. After conventional treatment, the levels of serum IL-6, IL-1β, and TNF-α were decreased by 18.3%, 44.5%, and 23.5%, respectively, and the difference was statistically significant. After PTL treatment, the serum of IL-6, IL-1β, and TNF-α were decreased by 82%, 58.6%, and 35%, respectively. After Nano PTL treatment, the serum IL-6, IL-1β, and TNF-α was decreased by 97.4%, 79.7% and 64.3%, respectively. The results showed that Nano PTL could more significantly inhibit the release of inflammatory cytokines (Figure 2C–E).

The levels of AST, ALT, Urea and Crea in the sepsis group were significantly increased. Compared with the conventional treatment, the levels of AST and ALT in the PTL group were further decreased. Compared with the PTL group, Nano PTL had better effects on AST and ALT (Figure 2F–I). The results suggest that Nano PTL can significantly improve the liver and kidney function during sepsis disease (Figure 2H and I).

The mean arterial pressure of the rats in the sepsis group was decreased. Conventional treatment slightly increased the MAP. PTL and Nano PTL significantly increased the mean arterial pressure as compared to the conventional treatment. Nano PTL had better effect (Figure 2J).

## Nano PTL Improved Sepsis-Induced Intestinal Barrier Dysfunction

The intestinal barrier function was severely impaired after sepsis. HE staining results showed that the structure of the intestine was impaired after sepsis, which was characterized by columnar epithelium necrosis, intestinal villus ruptured, and inflammatory cells and red blood cells infiltrated. Compared with the sepsis group, the structure of intestinal villus in the Nano PTL group was close to that of the normal group (Figure 3A). The EB leakage of intestine in sepsis rats was significantly increased. PTL and Nano PTL treatment significantly decreased the EB leakage of intestine as compared to the conventional treatment group, which were decreased by 38% and 68.6%, respectively (Figure 3B and C).

D-Lactic acid is the product of bacterial metabolism and glycolysis in the intestinal tract, and is an important indicator reflecting the function of the intestinal barrier. The results showed that compared with the normal control group, the concentration of blood D-lactic acid in the sepsis group was increased by 93.5%. Compared with the sepsis group, the

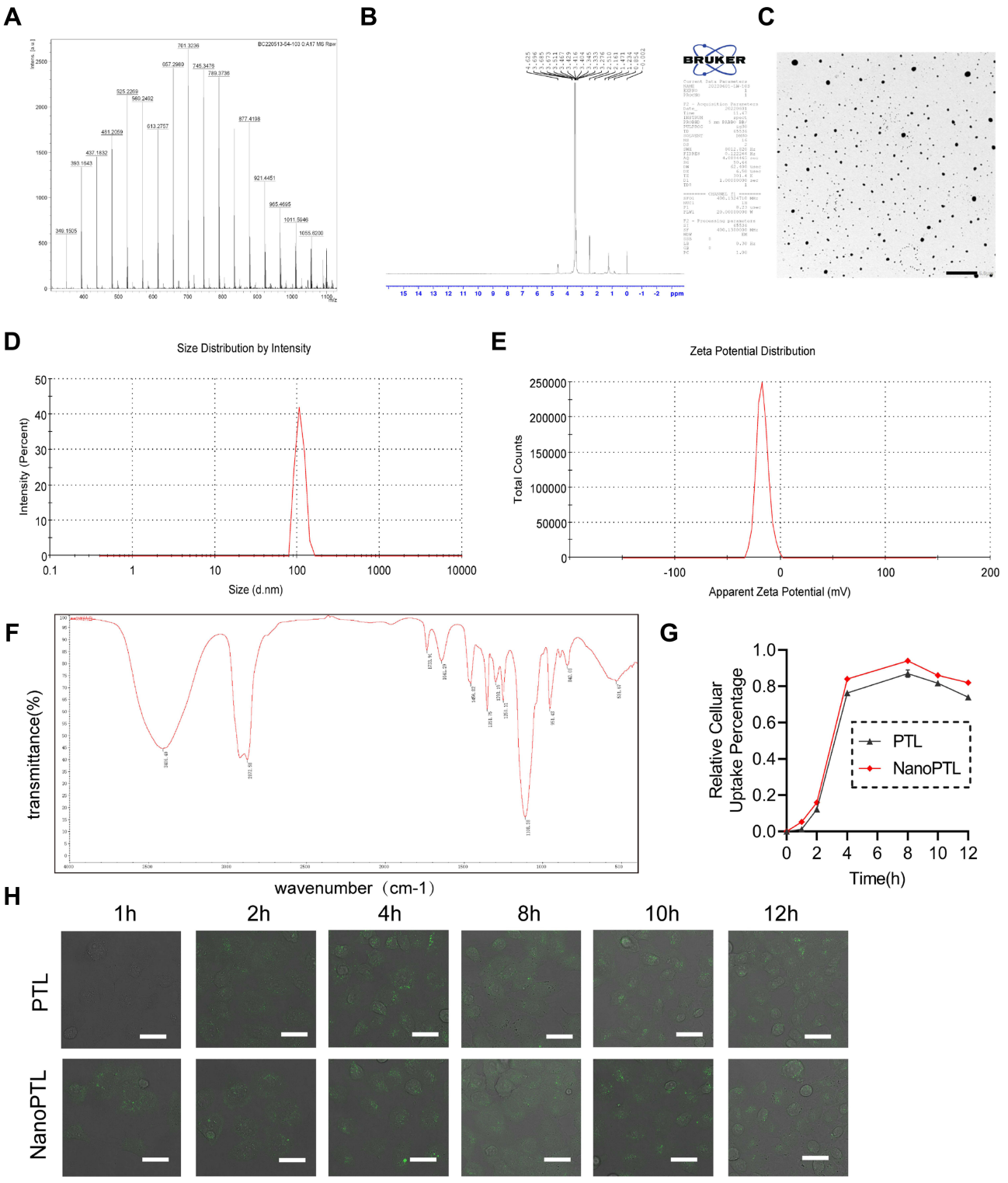


**Figure 1** Characterization of Nano PTL. (**A**) LC-MS spectrum of Nano PTL. (**B**) Nuclear magnetic resonance hydrogen spectrum of Nano PTL. (**C**) Representative image of TEM of Nano PTL (bar, 1 μm). (**D**) Size distribution of Nano PTL (n=3 independent experiments). (**E**) Zeta potential of Nano PTL (n=3 independent experiments). (**F**) Infrared spectroscopy of Nano PTL. (**G**) Uptake rates of PTL and Nano PTL by intestinal epithelial cells (n=3 independent experiments). (**H**) Uptake of FITC by intestinal epithelial cells at each time point (n=3 independent experiments, bar, 40 μm).

concentration of blood D-lactic acid in the conventional treatment group was decreased 52.8%. PTL and nano PTL further decreased the blood D-lactic acid, which was decreased by 62.1% and 79.5%, respectively, as compared with the conventional treatment group. (Figure 3D).

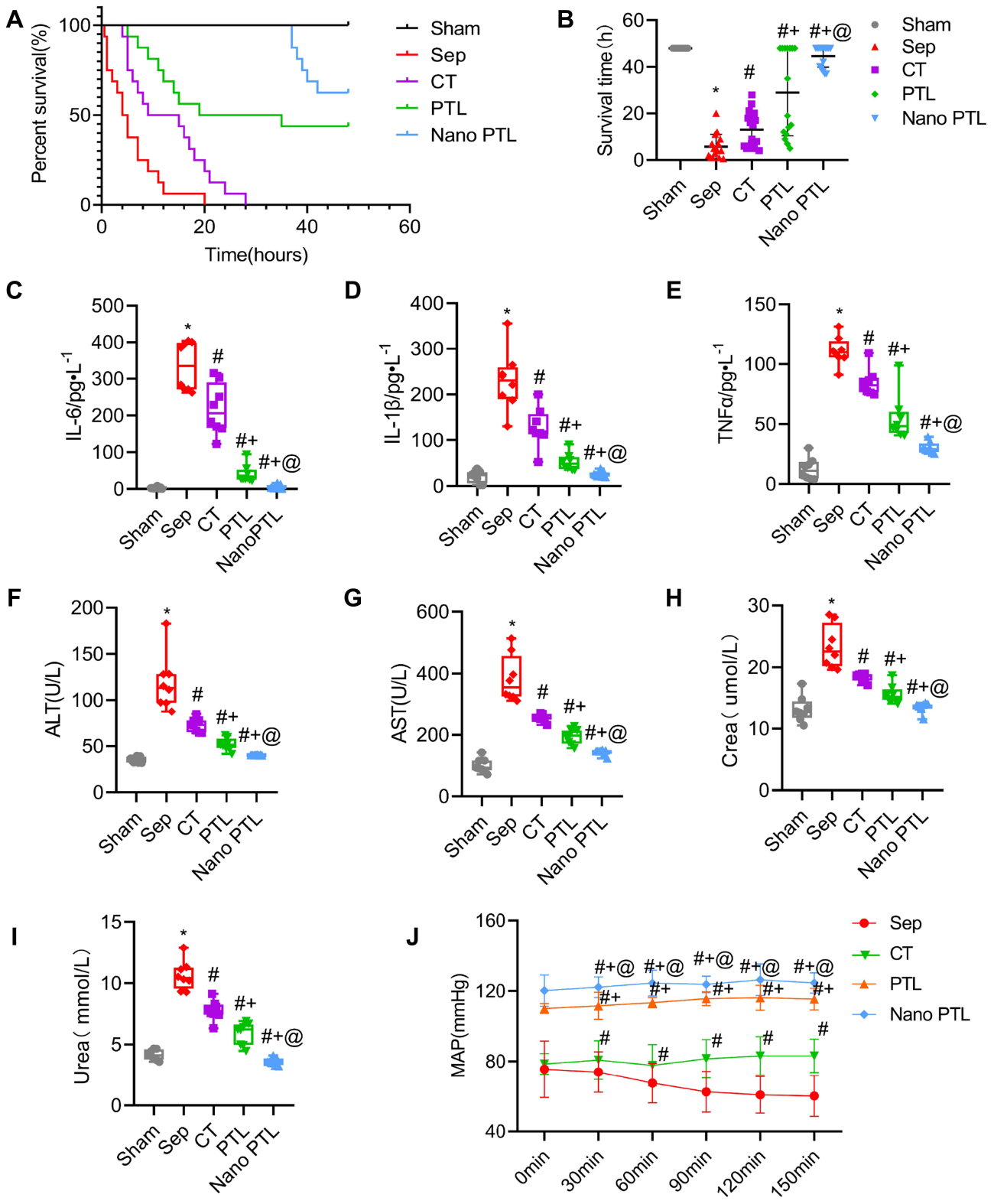


**Figure 2** Protective effect of Nano PTL on sepsis rats. (**A**) Survival rate. (**B**) Survival time of each group (n=16 per group). Effects of Nano PTL on (**C**) IL-6, (**D**) IL-1β and (**E**) TNF-α level (n=8 per group). Effects of Nano PTL on (**F**) ALT, (**G**)AST, (**H**) Crea and (**I**) Urea level (n=8 per group). (**J**) Mean arterial pressure of septic rats (n=8 per group). *P<0.05, compared with the Sham group. #P<0.05, compared with the Sep group. +P<0.05, compared with CT group. @P<0.05, compared with the PTL group.

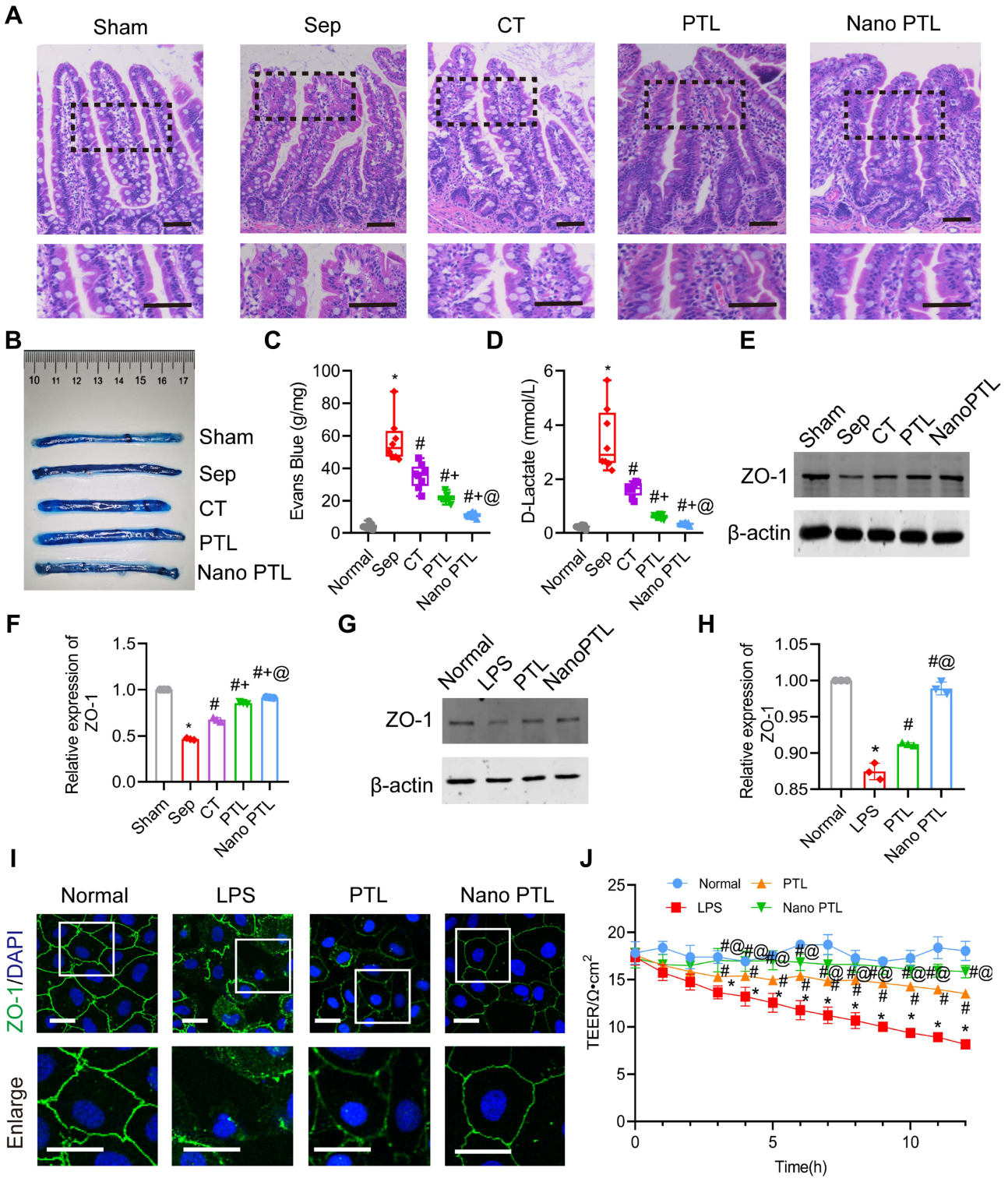


**Figure 3** Protective effect of Nano PTL on intestinal barrier function in septic rats. (**A**) Representative microphotographs of HE staining in intestine (bar, 100 μm, n=8 per group). (**B** and **C**) EB leakage of intestine after treated with Nano PTL (n=8 per group). (**D**) D-Lactic acid level in septic rats (n=8 per group). (**E** and **F**) Relative expression of ZO-1 intestinal tissues of rats (n=3 independent experiments). (**G** and **H**) Relative expression of ZO-1 in intestinal epithelial cells (n=3 independent experiments). (**I**) Representative immunofluorescence image of ZO-1 of intestinal epithelial cell (bar, 20 μm, n=3 independent experiments). (**J**) Effect of Nano PTL on TEER (n=3 independent experiments). *P<0.05, compared with the Sham group or Normal group. #P<0.05, compared with the Sep group or LPS group. +P<0.05, compared with the CT group. @P<0.05, compared with the PTL group.

Western blot results showed that the expression of ZO-1 in the LPS or sepsis group was significantly decreased, PTL and Nano PTL significantly increased the protein expression of ZO-1 (Figure 3E–H). Immunofluorescence results showed that the ZO-1 junctions of intestinal epithelial cells in the normal group were tightly connected. After LPS stimulation, the expression of ZO-1 showed discontinuous point-like, scattered distribution, and scattered in cells. After PTL and Nano PTL treatment, the expression of ZO-1 in intestinal epithelial cells was increased, the distribution of ZO-1 was roughly linear, Nano PTL had better effect (Figure 3I). The results of the TEER of intestinal epithelial cells in the normal group did not change. LPS stimulation and significantly decreased the TEER. Ordinary PTL and Nano PTL significantly increase the TEER, and Nano PTL had better effect (Figure 3J).

## Network Pharmacology Predicts the Target of PTL

In order to clarify the mechanism of PTL playing protective effect on sepsis, the potential targets were screened. We found 100 targets of PTL from the Swiss Target Prediction database (Figure 4A). In addition, we used the Genecards database, and got 2984 targets, the screening score of 62 targets was >5 (Supplementary Table 1). There were 41 intersections obtained by the Venn diagram (Figure 4B). Forty-one potential targets of PTL on sepsis were enriched for KEGG pathways (Figure 4C), and two of them were selected: Inflammatory mediator regulation of TRP channels and gap junction. Two common targets, 5-HTR2A and PKC, were selected for further analysis (Figure 4D). Western blot result showed that PTL had a significant effect on 5-HTR2A but had no effect on PKC. (Figure 4E).

## Nano PTL Inhibits Apoptosis and ROS Through 5-HTR2A

Combined with the results of network pharmacology, we further investigated whether PTL exerted a protective effect through the 5-HTR2A. Previous studies have reported that 5-HTR2A has a regulatory effect on apoptosis and oxidative stress. The present study found that in the LPS group, the levels of ROS, Bax, CytC and cleaved-Caspase3 in intestinal epithelial cells were significantly enhanced. After being treated with PTL and Nano PTL, the levels of ROS, Bax, CytC and cleaved-Caspase3 were significantly decreased, Nano PTL had better effects on these parameters (Figure 5A–E). Flow cytometry observation showed that the apoptosis of intestinal epithelial cells was significantly increased in the LPS group as compared with the normal group. PTL and Nano PTL treatment significantly decreased the apoptosis of intestinal epithelial cells (Figure 5F). 5-HTR2A inhibitor significantly antagonized the effect of Nano PTL on ROS production and apoptosis of intestinal epithelial cells (Figure 5A–F). The results of TEER showed that 5-HTR2A inhibitor could antagonize the protective effect of Nano PTL on intestinal barrier leakage of (Figure 5G). These results confirmed that Nano PTL exerts the protective effect on intestinal barrier function mainly through the 5-HTR2A.

# Discussion

Sepsis can cause the intestinal barrier damage and dysfunction, leading to the translocation of intestinal flora, which can aggravate the severity of sepsis and uncontrolled inflammatory response, and multiple organ failure, eventually leading to death.[21] Sepsis-induced intestinal barrier function damage was mainly related to the destruction of intestinal mucosal cell and the tight junction of cell to cell.[22] Cecal ligation and puncture (CLP) is a commonly used model of trauma, infection and stress reaction. A large number of gram-negative bacteria can release endotoxin into the blood, causing sepsis and inducing systemic inflammatory reaction and metabolic disorder,[23] but no effective treatment measures are available at present. In order to search for effective method to protect the intestinal barrier function of sepsis, Nano PTL was synthesized, and its protective effect on the intestinal barrier function with CLP-induced sepsis rat model was observed. The results showed that at the same concentration, Nano PTL had better effects on the intestinal barrier than PTL. Besides, Nano PTL could protect the organ function, and increase the survival rate and survival time of sepsis rats. The mechanism is closely related to its inhibition on cell apoptosis and oxidative stress through 5-HTR2A (Figure 5H).

The intestine is considered to be the "central organ" of multiple organ failure.[24] After sepsis, the intestinal permeability is increased, which can cause the intestinal bacteria and endotoxins translocation to aggravate sepsis.[25] Previous studies have found that PTL can mediate the production of SCFAs (short-chain fatty acids) by increasing the metabolites, improve the balance of Treg/Th17 in the intestinal mucosa, and improve colonic inflammation.[26] PTL can

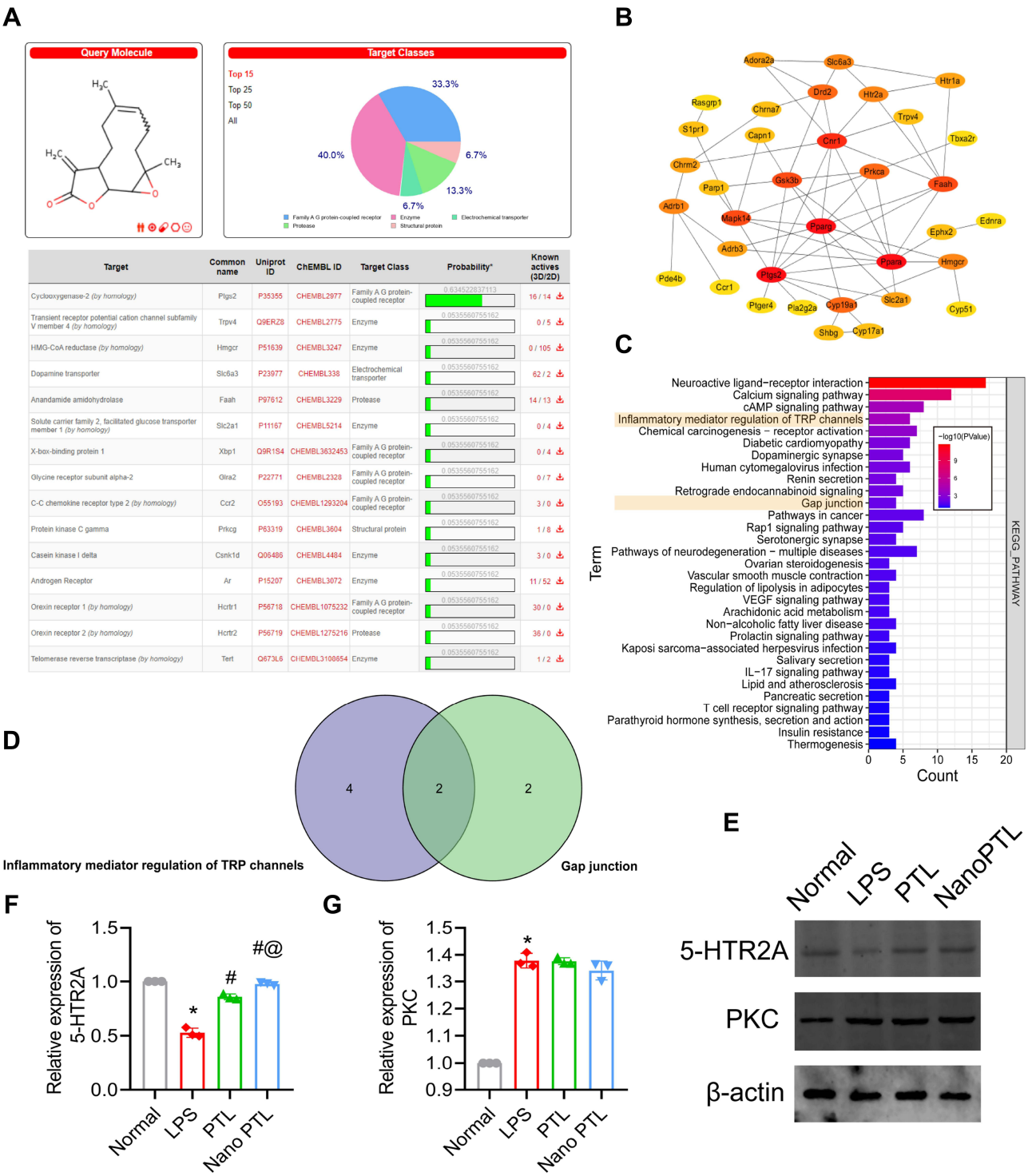


| Target | Common name | Uniprot ID | ChEMBL ID | Target Class | Probability* | Known actives (3D/2D) |
|---|---|---|---|---|---|---|
| Cyclooxygenase-2 *(by homology)* | Ptgs2 | P35355 | CHEMBL2977 | Family A G protein-coupled receptor | 0.634522837113 | 16 / 14 |
| Transient receptor potential cation channel subfamily V member 4 *(by homology)* | Trpv4 | Q9ERZ8 | CHEMBL2775 | Enzyme | 0.0535560755162 | 0 / 5 |
| HMG-CoA reductase *(by homology)* | Hmgcr | P51639 | CHEMBL3247 | Enzyme | 0.0535560755162 | 0 / 105 |
| Dopamine transporter | Slc6a3 | P23977 | CHEMBL338 | Electrochemical transporter | 0.0535560755162 | 62 / 2 |
| Anandamide amidohydrolase | Faah | P97612 | CHEMBL3229 | Protease | 0.0535560755162 | 14 / 13 |
| Solute carrier family 2, facilitated glucose transporter member 1 *(by homology)* | Slc2a1 | P11167 | CHEMBL5214 | Enzyme | 0.0535560755162 | 0 / 4 |
| X-box-binding protein 1 | Xbp1 | Q9R1S4 | CHEMBL3632453 | Family A G protein-coupled receptor | 0.0535560755162 | 0 / 4 |
| Glycine receptor subunit alpha-2 | Glra2 | P22771 | CHEMBL2328 | Family A G protein-coupled receptor | 0.0535560755162 | 0 / 7 |
| C-C chemokine receptor type 2 *(by homology)* | Ccr2 | O55193 | CHEMBL1293204 | Family A G protein-coupled receptor | 0.0535560755162 | 3 / 0 |
| Protein kinase C gamma | Prkcg | P63319 | CHEMBL3604 | Structural protein | 0.0535560755162 | 1 / 8 |
| Casein kinase I delta | Csnk1d | Q06486 | CHEMBL4484 | Enzyme | 0.0535560755162 | 3 / 0 |
| Androgen Receptor | Ar | P15207 | CHEMBL3072 | Enzyme | 0.0535560755162 | 11 / 52 |
| Orexin receptor 1 *(by homology)* | Hcrtr1 | P56718 | CHEMBL1075232 | Family A G protein-coupled receptor | 0.0535560755162 | 30 / 0 |
| Orexin receptor 2 *(by homology)* | Hcrtr2 | P56719 | CHEMBL1275216 | Protease | 0.0535560755162 | 36 / 0 |
| Telomerase reverse transcriptase *(by homology)* | Tert | Q673L6 | CHEMBL3100654 | Enzyme | 0.0535560755162 | 1 / 2 |

**Figure 4** Network pharmacology predicts the action target of PTL. (**A**) Target gene of PTL obtained from Swiss target prediction. (**B**) Target gene of PTL on Sepsis. (**C**) KEGG enrichment pathway. (**D**) Venn diagram. (**E**) Western blot of 5-HTR2A and PKC in intestinal epithelial cells after treated with Nano PTL (n=3 independent experiments). (**F** and **G**) The relative expressions of 5-HTR2A and PKC (n=3 independent experiments). *P<0.05, compared with Normal. $^{\#}$P<0.05, compared with the LPS group. $^{@}$P<0.05, compared with the PTL group.

also inhibit NF-κB and oxidative stress, and its inhibitory activity is mediated by the unsaturated carbonyl structure.[27] In this study, we found that Nano PTL can protect the intestinal barrier function of sepsis rats by inhibiting intestinal epithelial cells' apoptosis and oxidative stress.

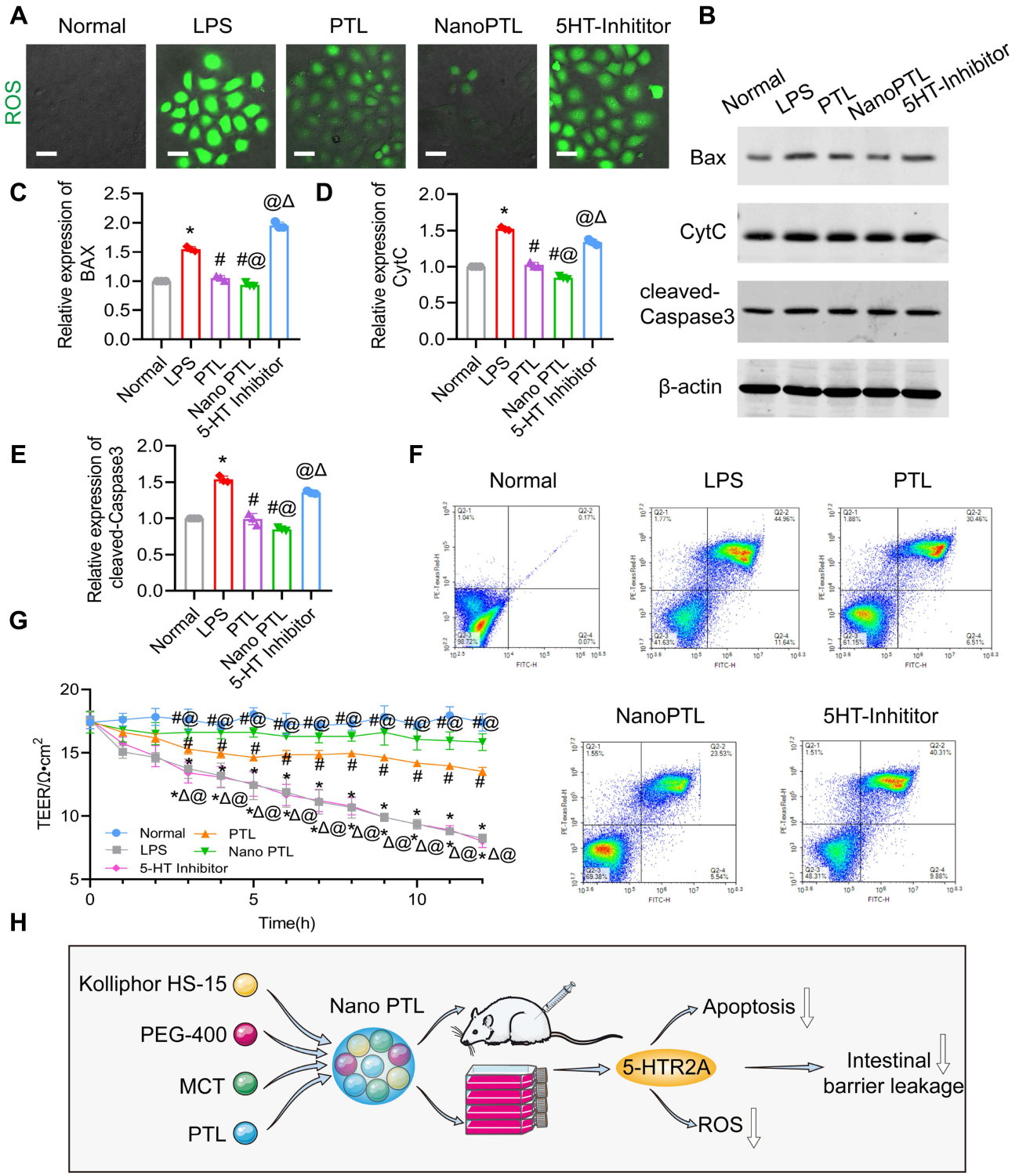


**Figure 5** Protective effect of Nano PTL on ROS and apoptosis of intestinal epithelial cells through 5-HTR2A. (**A**) ROS level of intestinal epithelial cells (bar, 20 μm, n=3 independent experiments). (**B**) The effect of Nano PTL on the expression of apoptosis-related proteins Bax, CytC and cleaved-Caspase3 (n=3 independent experiments). Analysis of relative expressions of (**C**) Bax, (**D**) CytC, and (**E**) cleaved-Caspase3. (**F**) Flow cytometry of apoptosis. (**G**) Effect of 5HT-Inhibitor on TEER (n=3 independent experiments). (**H**) The schematic diagram for the mechanism of the therapeutic effect of Nano PTL on intestinal barrier function after sepsis. *P<0.05, compared with Normal. #P<0.05, compared with the LPS group. @P<0.05, compared with the PTL group ΔP<0.05, compared with the Nano PTL group.

Nano-drugs have broad application prospects. It has been reported that targeting nano-curcumin can improve bioavailability and gingival inflammation.[28] Low-dose nano-drugs can reduce the aggregation of inflammatory cells to improve inflammation and reduce cytotoxicity.[29] Nano-sized peroxidase has higher stability and anti-inflammatory

activity.[30] Literature showed that Nano-sized curcumin could improve its biological safety and inhibit inflammation and apoptosis of pancreatic islet B cells.[31] In this study, Nano PTL was synthesized using a Kolliphor HS-15, MCT with PEG and PTL. The size of Nano PTL was correlated with in vivo size of biomacromolecules (such as proteins, nucleic acids, etc), it is far smaller than the size of various organelles. So nano PTL can improve the bioavailability of PTL and cell uptake, which can enable it to achieve long-term circulation features. Most inflammatory cells have rich lysosomes, mitochondria, and rough endoplasmic reticulum. Nano PTL can increase the accumulation of PTL in inflammatory cells and increase the concentration of PTL in the acting cells to achieve good effects of anti-inflammation. But in the process of drug uptake by cells through endocytosis, the fluorescence life of donors will be shortened. When endocytosis vesicles release drugs in cells, the distance between cell membrane and drugs changes, and the fluorescence effect weakens or disappears.[32] Our present study showed that nanosizing of PTL increased the bioavailability and cell uptake rate of PTL, increasing the protective effects.

Previous studies have found that PTL can inhibit apoptosis by reducing the activation of p53.[33] In this study, we found that PTL acts on 5-HTR2A gene through network pharmacology to inhibit cell death. We used cecal ligation and puncture and LPS stimulation to replicate the septic rat model in vivo and in vitro. PTL was modified to improve its drug loading. The target was identified by network pharmacology, and the mechanism of PTL was found to be related to 5-HTR2A gene via in vivo and in vitro experiments. Programmed cell death can eliminate unnecessary or diseased cells in the body and play an important role in maintaining the normal function of cells in the body.[34] Excessive activation of apoptosis can also lead to organ damage. It has been found that mtDNA activates the cGAS-STING-IRF3 pathway, induces the production of pro-inflammatory factors and IFN, and promotes the apoptosis of intestinal epithelial cells during sepsis, which leads to intestinal barrier damage in sepsis.[35] Enhanced function of the Cx43 channel during sepsis can lead to increased generation of ROS, activate the JNK1/Sirt1/FoxO3a signaling pathway, further promote the activation of downstream target genes BIM and PUMA, and promote cell apoptosis.[36] Studies have shown that 5-HTR2A can reduce the activation of endoplasmic reticulum stress and reduce the increase of ROS. We found that PTL could reduce oxidative stress levels through 5-HTR2A. In addition, some studies have found that 5-HTR2A inhibits the phosphatidylinositol-3 kinase PI3K/Akt and ERK1/2 signalling pathways by inhibiting the production of ROS, thereby down-regulating IκB, inhibiting the production of NF-κB, inhibiting apoptosis.[37] Recent studies have found that the down-regulation of 5-HTR2A in the brain can lead to cell apoptosis.[38] The binding of 5-HTR2A to its receptors can activate the PI3K/Akt pathway in cells, inhibit Bax/Bcl2 from forming holes in the mitochondrial membrane, and prevent apoptosis.[39] 5-HTR2A can activate ERK1/2 by increasing the level of p-ERK1/2 and increasing the expression of Bcl-3 to inhibit apoptosis.[40] Previous research found that the Shh-Nkx2-2-Lmx1b-Pet1 cascade can occur when 5-HTR2A levels are severely decreased, then activates the ERK pathway and promotes 5-HTR2A synthesis in the CNS to inhibit apoptosis. Some studies have reported that PTL can prevent migraine by inhibiting 5-HTR2A.[41] This study found that Nano PTL can inhibit the production of cell apoptotic factors, reduce the level of apoptosis, reduce oxidative stress, and play a protective effect on intestinal barrier of sepsis rats by up-regulating the 5-HTR2A.

## Conclusion

The above results show that, compared with ordinary PTL, Nano PTL further reduces the intestinal permeability and protects the intestinal barrier function in sepsis rats. The mechanism may be related to the 5-HTR2A signal regulation pathway. Whether Nano PTL has the same effect in large animals and human sepsis also needs further research to clarify. In order to achieve better drug treatment effects, in addition to controlling the particle size of nano-drugs, targeting ligands can also be modified outside the nano-carriers in the future, and the combined use of the two strategies may achieve better results.

## Abbreviations

PTL, parthenolide; Nano PTL, nano parthenolide; TEER, transmembrane resistance; ROS, reactive oxygen species; CT, conventional treatment; CLP, cecal ligation and puncture; LPS, lipopolysaccharide; 5-HTR2A, serotonin 2A; ICU, Intensive Care Unit; SOD, superoxide dismutase; CAT, chloramphenicol acetyltransferase; MDA, malondialdehyde; ATP, Adenosine-triphosphate; MAP, mean arterial blood pressure; Cytc, cytochrome; BBB, blood–brain barrier; DSS,

dextran sodium sulfate; PKC, protein kinase C; ZO-1, zonula occludens-1; Bax, BCL2-associated X; Cytc, cytochrome; AST, aspartate aminotransferase; ALT, alanine aminotransferase; Crea, creatinine; Urea, urea nitrogen; PEG, polyethylene glycol; MCT, medium-chain triglycerides; NETs, extraneutrophiltraps; ZP, zeta potential; PDI, polydispersity index; TEM, transmission electron microscope; FITC, fluoresceinIsothiocyanate, IECS, intestinal epithelial cells; CNS, central nervous system; SCFAs, short-chain fatty acids; IL-6, interleukin-6; IL-1β, interleukin-1β; TNF-α, tumor necrosis factor-α; PBS, phosphate-buffered saline.

## Data Sharing Statement

The raw data of this study are available from the corresponding author on reasonable request.

## Ethics Approval and Consent to Participate

The ethics and the protocols for the animal experiments were approved by the Ethical Committee of Army Medical University.

## Author Contributions

All authors made a significant contribution to the work reported, whether that is in the conception, study design, execution, acquisition of data, analysis and interpretation, or in all these areas; took part in drafting, revising or critically reviewing the article; gave final approval of the version to be published; have agreed on the journal to which the article has been submitted; and agree to be accountable for all aspects of the work.

## Funding

This study was supported by the Key Program of the National Natural Science Foundation of China (No.81730059) and the Key Program of the National Natural Science Foundation of China (No.81830065). National Natural Science Foundation of China (No. 82270523). Chongqing Postgraduate Research and Innovation Project (No. GYB22285).

## Disclosure

The authors report no conflicts of interest in this work.

## References

1. Rudd KE, Johnson SC, Agesa KM, et al. Global, regional, and national sepsis incidence and mortality, 1990–2017: analysis for the global burden of disease study. *Lancet*. 2020;395(10219):200–211. doi:10.1016/S0140-6736(19)32989-7
2. Rajaee A, Barnett R, Cheadle WG. Pathogen- and danger-associated molecular patterns and the cytokine response in sepsis. *Surg Infect*. 2018;19(2):107–116. doi:10.1089/sur.2017.264
3. Wang C, Li Q, Ren J. Microbiota-immune interaction in the pathogenesis of gut-derived infection. *Front Immunol*. 2019;10:1873. doi:10.3389/fimmu.2019.01873
4. Peng Z, Niu Z, Zhang R, et al. Antimicrobial step-down therapy versus conventional antimicrobial therapy in the treatment of patients with sepsis. *Dis Markers*. 2022;2022:3117805. doi:10.1155/2022/3117805.eCollection2022
5. Dong Y, Qian X, Li J. Sesquiterpene lactones and cancer: new insight into antitumor and anti-inflammatory effects of parthenolide-derived dimethylaminomicheliolide and micheliolide. *Comput Math Methods Med*. 2022;2022:3744837. doi:10.1155/2022/3744837
6. Wang D, Wang H, Fu S, et al. Parthenolide ameliorates concanavalin A-induced acute hepatitis in mice and modulates the macrophages to an anti-inflammatory state. *Int Immunopharmacol*. 2016;38:132–138. doi:10.1016/j.intimp.2016.05.024
7. Zhang Y, Miao L, Peng Q, et al. Parthenolide modulates cerebral ischemia-induced microglial polarization and alleviates neuroinflammatory injury via the RhoA/ROCK pathway. *Phytomedicine*. 2022;105:154373. doi:10.1016/j.phymed.2022.154373
8. CuiZ-Y, Wang G, Zhang J, et al. Parthenolide, bioactive compound of Chrysanthemum parthenium L., ameliorates fibrogenesis and inflammation in hepatic fibrosis via regulating the crosstalk of TLR4 and STAT3 signaling pathway. *Phytother Res*. 2021;35(10):5680–5693. doi:10.1002/ptr.7214
9. Dong L, Qiao H, Zhang X, et al. Parthenolide is neuroprotective in rat experimental stroke model: downregulating NF-κB, phospho-p38MAPK, and caspase-1 and ameliorating BBB permeability. *Mediators Inflamm*. 2013;2013:370804. doi:10.1155/2013/370804
10. Sheehan M, Wong HR, Hake PW, Zingarelli B. Parthenolide improves systemic hemodynamics and decreases tissue leukosequestration in rats with polymicrobial sepsis. *Crit Care Med*. 2003;31(9):2263–2270. doi:10.1097/01.CCM.0000085186.14867.F7
11. Kim SL, Liu YC, Seo SY, et al. Parthenolide induces apoptosis in colitis-associated colon cancer, inhibiting NF-κB signaling. *Oncol Lett*. 2015;9(5):2135–2142. doi:10.3892/ol.2015.3017
12. Sun R, Dai J, Ling M, et al. Delivery of triptolide: a combination of traditional Chinese medicine and nanomedicine. *J Nanobiotechnology*. 2022;20(1):194. doi:10.1186/s12951-022-01389-7

13. Zewail M, Gaafar E, Ali MM, Abbas H. Lipidic cubic-phase leflunomide nanoparticles (cubosomes) as a potential tool for breast cancer management. *Drug Deliv*. 2022;29(1):1663–1674. doi:10.1080/10717544.2022.2079770
14. Xi J, Fang JH, Xiong XM, et al. Acid water-ground nano-realgar is superior to crude realgar in promoting apoptosis of MCF-7 breast cancer cells. *Curr Med Sci*. 2022;42(4):720–732. doi:10.1007/s11596-022-2605-5
15. Wang C, Li F, Zhang T, Yu M, Sun Y. Recent advances in anti-multidrug resistance for nano-drug delivery system. *Drug Deliv*. 2022;29 (1):1684–1697. doi:10.1080/10717544.2022.2079771
16. Salatin S, Yari Khosroushahi A. Overviews on the cellular uptake mechanism of polysaccharide colloidal nanoparticles. *J Cell Mol Med*. 2017;21 (9):1668–1686. doi:10.1111/jcmm.13110
17. Sadegha S, Varshochian R, Dadras P, et al. Mesoporous silica coated SPIONs containing curcumin and silymarin intended for breast cancer therapy. *Daru*. 2022;30(2):331–341. doi:10.1007/s40199-022-00453-9
18. She H, Hu Y, Zhou Y, et al. Protective effects of dexmedetomidine on sepsis-induced vascular leakage by alleviating ferroptosis via regulating metabolic reprogramming. *J Inflamm Res*. 2021;14:6765–6782. doi:10.2147/JIR.S340420
19. Zhu HJ, Wang JS, Markowitz JS, Donovan JL, Gibson BB, DeVane CL. Risperidone and paliperidone inhibit p-glycoprotein activity in vitro. *Neuropsychopharmacology*. 2007;32(4):757–764. doi:10.1038/sj.npp.1301181
20. Zheng D, Zhou H, Wang H, et al. Mesenchymal stem cell-derived microvesicles improve intestinal barrier function by restoring mitochondrial dynamic balance in sepsis rats. *Stem Cell Res Ther*. 2021;12(1):299. doi:10.1186/s13287-021-02363-0
21. Greco E, Lupia E, Bosco O, Vizio B, Montrucchio G. Platelets and multi-organ failure in sepsis. *Int J Mol Sci*. 2017;18(10):2200. doi:10.3390/ijms18102200
22. Fay KT, Ford ML, Coopersmith CM. The intestinal microenvironment in sepsis. *Biochim Biophys Acta Mol Basis Dis*. 2017;1863(10 Pt B):2574–2583. doi:10.1016/j.bbadis.2017.03.005
23. Huang M, Cai S, Su J. The pathogenesis of sepsis and potential therapeutic targets. *Int J Mol Sci*. 2019;20(21):5376. doi:10.3390/ijms20215376
24. Li H, Xie J, Guo X, et al. Bifidobacterium spp. and their metabolite lactate protect against acute pancreatitis via inhibition of pancreatic and systemic inflammatory responses. *Gut Microbes*. 2022;14(1):2127456. doi:10.1080/19490976.2022.2127456
25. Cigarran Guldris S, González Parra E, Cases Amenós A. Gut microbiota in chronic kidney disease. Microbiota intestinal en la enfermedad renal crónica. *Nefrologia*. 2017;37(1):9–19. doi:10.1016/j.nefro.2016.05.008
26. Xu S, Li L, Wu J, et al. Melatonin attenuates sepsis-induced small-intestine injury by upregulating SIRT3-mediated oxidative-stress inhibition, mitochondrial protection, and autophagy induction. *Front Immunol*. 2021;12:625627. doi:10.3389/fimmu.2021.625627
27. Tsai TY, Chan P, Gong CL, et al. Parthenolide-induced cytotoxicity in H9c2 cardiomyoblasts involves oxidative stress. *Acta Cardiol Sin*. 2015;31 (1):33–41. doi:10.6515/acs20140422b
28. Malekzadeh M, Kia SJ, Mashaei L, Moosavi MS. Oral nano-curcumin on gingival inflammation in patients with gingivitis and mild periodontitis. *Clin Exp Dent Res*. 2021;7(1):78–84. doi:10.1002/cre2.330
29. de Oliveira Carvalho H, Gonçalves D, Picanço K, et al. Actions of Cannabis sativa L. fixed oil and nano-emulsion on venom-induced inflammation of Bothrops moojeni snake in rats. *Inflammopharmacology*. 2021;29(1):123–135. doi:10.1007/s10787-020-00754-y
30. Al-Hazmi NE, Naguib DM. Nano-peroxidase a promising anti-inflammatory and antibacterial agent against bacteria and inflammation related to colorectal cancer. *J Gastrointest Cancer*. 2022;53(2):415–419. doi:10.1007/s12029-021-00626-w
31. Ganugula R, Arora M, Jaisamut P, et al. Nano-curcumin safely prevents streptozotocin-induced inflammation and apoptosis in pancreatic beta cells for effective management of type 1 diabetes mellitus. *Br J Pharmacol*. 2017;174(13):2074–2084. doi:10.1111/bph.13816
32. Botella P, Muniesa C, Vicente V, Cabrera-García A. Effect of drug precursor in cell uptake and cytotoxicity of redox-responsive camptothecin nanomedicines. *Mater Sci Eng C Mater Biol Appl*. 2016;58:692–699. doi:10.1016/j.msec.2015.09.012
33. Ren Y, Li Y, Lv J, et al. Parthenolide regulates oxidative stress-induced mitophagy and suppresses apoptosis through p53 signaling pathway in C2C12 myoblasts. *Cell Biochem*. 2019;120(9):15695–15708. doi:10.1002/jcb.28839
34. Li QS, Jia YJ. Ferroptosis: a critical player and potential therapeutic target in traumatic brain injury and spinal cord injury. *Neural Regen Res*. 2023;18(3):506–512. doi:10.4103/1673-5374.350187
35. Hu Q, Ren H, Li G, et al. STING-mediated intestinal barrier dysfunction contributes to lethal sepsis. *EBioMedicine*. 2019;41:497–508. doi:10.1016/j.ebiom.2019.02.055
36. Zou Z, Liu B, Zeng L, et al. Cx43 inhibition attenuates sepsis-induced intestinal injury via downregulating ROS transfer and the activation of the JNK1/Sirt1/FoxO3a signaling pathway. *Mediators Inflamm*. 2019;2019:7854389. doi:10.1155/2019/7854389
37. Zha L, Chen J, Sun S, et al. Soyasaponins can blunt inflammation by inhibiting the reactive oxygen species-mediated activation of PI3K/Akt/NF-kB pathway. *PLoS One*. 2014;9(9):e107655. doi:10.1371/journal.pone.0107655
38. Mohammadi A, Rashidi E, Amooeian VG. Brain, blood, cerebrospinal fluid, and serum biomarkers in schizophrenia. *Psychiatry Res*. 2018;265:25–38. doi:10.1016/j.psychres.2018.04.036
39. Borkowski LF, Smith CL, Keilholz AN, Nichols NL. Divergent receptor utilization is necessary for phrenic long-term facilitation over the course of motor neuron loss following CTB-SAP intrapleural injections. *Neurophysiol*. 2021;126(3):709–722. doi:10.1152/jn.00236.2021
40. Zhao H, Chen S, Hu K, et al. 5-HTP decreases goat mammary epithelial cells apoptosis through MAPK/ERK/Bcl-3 pathway. *Gene*. 2021;769:145240. doi:10.1016/j.gene.2020.145240
41. Takeshima T, Komori M, Tanji Y, Ozeki A, Tatsuoka Y. Efficacy of lasmiditan across patient and migraine characteristics in Japanese patients with migraine: a secondary analysis of the MONONOFU trial. *Adv Ther*. 2022;39(11):5274–5288. doi:10.1007/s12325-022-02304-0